

Hyperspectral remote sensing of atmospheric profiles from satellites and aircraft

W. L. Smith^a, D.K. Zhou^a, F.W. Harrison^a, H.E. Revercomb^b, A.M. Larar^a, A.H. Huang^b, B.Huang^b,

^aNASA Langley Research Center, 100 NASA Road, Hampton, VA 23681-2199

^bUniversity of Wisconsin, 1225 W. Dayton Street, Madison, WI 53706

Abstract

A future hyperspectral resolution remote imaging and sounding system, called the GIFTS, is described. An airborne system, which produces the type of hyperspectral resolution sounding data to be achieved with the GIFTS, has been flown on high altitude aircraft. Results from simulations and from the airborne measurements are presented to demonstrate the revolutionary remote sounding capabilities to be realized with future satellite hyperspectral remote imaging/sounding systems.

1. Introduction

A new era is about to begin in hyperspectral remote sensing, namely the implementation of hyperspectral remote sounding systems. The Geostationary Imaging Fourier Transform Spectrometer (GIFTS), selected for flight demonstration as NASA's New Millennium Program Earth Observing-3 (EO-3) Mission, combines new and emerging sensor and data processing technologies to acquire geophysical measurements that lead to revolutionary improvements in meteorological observations and forecasting. The GIFTS uses a large area format focal plane detector array (128 x 128) in a Fourier Transform Spectrometer (FTS)^{1,2} mounted on a geostationary satellite to enable the simultaneous gathering of high spectral resolution (as great as 0.3 cm^{-1}) and high spatial resolution (4-km x 4-km pixel) Earth infrared radiance spectra over a large area (512-km x 512-km) of the Earth within a 10 second time interval. A low visible light level camera provides quasi-continuous imaging of clouds at 1-km spatial resolution. Extended Earth coverage is achieved by step scanning the instrument field of view in a contiguous fashion across any desired portion of the visible Earth. The radiance spectra observed at each time step are transformed to high vertical resolution (1-2 km) temperature and water vapor mixing ratio profiles using rapid profile retrieval algorithms. These profiles are obtained on a 4km grid and then converted to relative humidity profiles. Images of the horizontal distribution of relative humidity for atmospheric levels, vertically separated by approximately 2 km, are constructed for each spatial scan. The sampling period will range from minutes to an hour, depending upon the spectral resolution and the area coverage selected for the measurement. Successive images of clouds and the relative humidity for each atmospheric level are then animated to reveal the motion of small-scale thermodynamic features of the atmosphere, providing a measure of the wind velocity distribution as a function of altitude^{3,4}. The net result is a dense grid of temperature, moisture, and wind profiles which can also be used for atmospheric analyses and operational weather prediction. Feature tracking can be performed for mixing ratio profiles of O₃ and CO, derived from their spectral radiance features observed by the FTS instrument, providing a direct measure of the transport of these pollutant and greenhouse gases. It is the unique combination of the Fourier transform spectrometer and the large area format detector array (i.e., an imaging interferometer) and the geostationary satellite observation platform that enables the revolutionary wind profile and trace gas transport remote sensing measurements.

Copyright 2000 Society of Photo-Optical Instrumentation Engineers.

This paper was published in the proceedings of the SPIE, Second SEPI International Asia-Pacific Symposium on Remote Sensing of the Atmosphere, Environment, and Space, 9-12 October 2000; Sendai, Japan, and is made available as an electronic preprint with permission of SPIE. One print may be made for personal use only. Systematic or multiple reproduction, distribution to multiple locations via electronic or other means, duplication of any material in this paper for a fee or for commercial purposes, or modification of the content of the paper are prohibited.

2. The GIFTS Instrument

The optical layout of the GIFTS instrument is shown in Figure 1. The imaging FTS produces the interferometric patterns for spectral separation of scene radiation reaching the detector arrays. To limit the background signal, the FTS is thermally controlled at a low temperature. The high data rates generated by the focal plane arrays (FPAs) are reduced by loss-less compression techniques then passed to the telemetry system by low-power, low-volume next-generation electronic components.

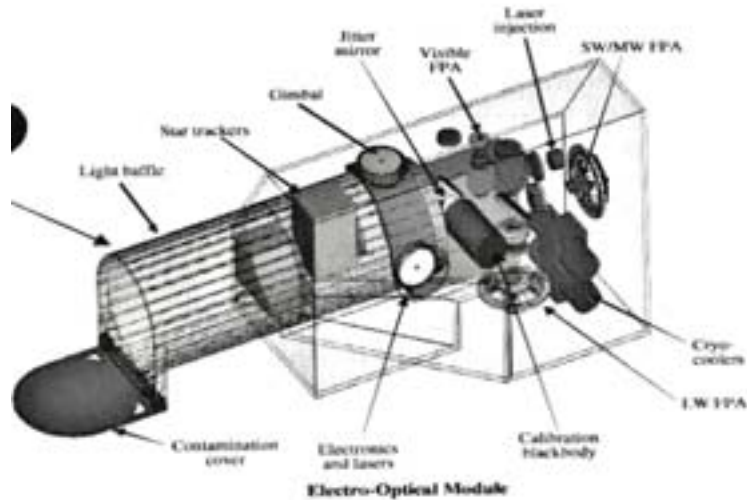


Figure 1. Schematic of GIFTS Optical Module

GIFTS will view areas of the Earth with a linear dimension of about 500-km, anywhere on the visible disk for a period between 0.125 and 25.0 sec, depending on the data application (i.e., imaging, sounding, or chemistry). GIFTS uses two detector arrays to cover the spectral bands, 685 to 1130 cm^{-1} and 1650 to 2250 cm^{-1} (Figure 2), within a Michelson interferometer to achieve a wide range of spectral resolutions (Table I).

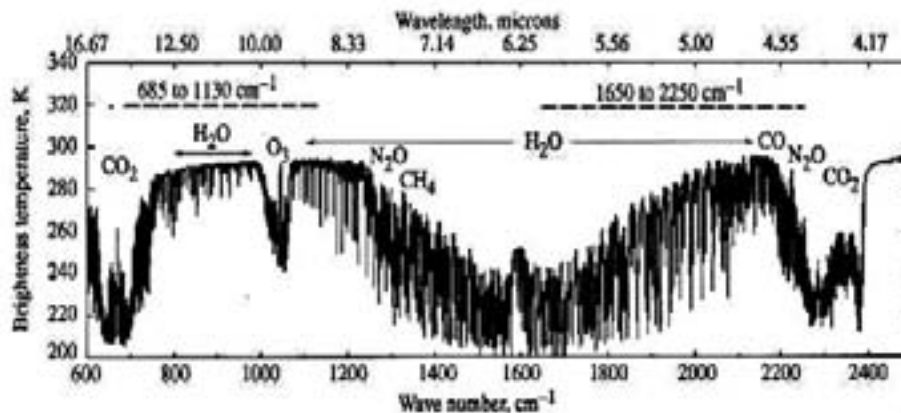


Figure 2: GIFTS spectral coverage with 2 detector arrays with spectral features of key radiatively active atmospheric trace gases.

These spectral characteristics achieve all technology/scientific validation objectives of GIFTS, as well as the sounding accuracy desired for a future operational sounding system. The Michelson interferometer, or

FTS, approach for geostationary satellite applications allows spectral resolution to be easily traded for greater area coverage or higher temporal resolution.

Table I: Five example GIFTS operating modes

Visible Resolution = 1 km; IR Resolution = 4 km

Mode	Resolution		Coverage	
	Spectral	OPD	Area	Time*
Stare Mode	0.3-36 cm ⁻¹	0.014-1.744 cm	512 km	<1-20 sec
Regional Imaging	36 cm ⁻¹	0.014 cm	6,000 km	3 min
Global Sounding	18 cm ⁻¹	0.027 cm	10,000 km	7 min
Regional Sounding and Chemistry	0.6 cm ⁻¹	0.872 cm	6000 km	25 min
Self Validation**	0.3 cm ⁻¹	1.744 cm	1000 km	60 min

Assumes a constant data rate associated with a Michelson mirror scan velocity of 0.17 cm/sec and 1 sec telescope pointing step time.
 ** Provides radiometric precision better than 0.1 K over all wavelengths

Table I shows the area coverage, measurement frequency, spectral resolution, and geophysical measurement for example modes of operation for GIFTS. Quasi-continuous imagery of localized areas and minute-interval imagery of large-scale areas can be achieved. Full disk sounding coverage will be obtained every 7 min at contemporary sounder spectral resolutions (e.g., 18 cm⁻¹). High vertical resolution soundings and atmospheric chemistry measurements of GIFTS require 0.6 cm⁻¹ spectral resolution and a longer stare time, thereby reducing the area coverage and/or frequency of observation relative to the imagery mode of operation. Nevertheless, GIFTS will cover a major portion of the visible disk with high vertical resolution soundings in less than 0.5 hour. This feature is important for obtaining wind profiles from geostationary temperature and moisture sounding data. A relatively long dwell time and a more limited area coverage “self validation mode” of operation will enable 0.3-cm⁻¹ spectral resolution radiances to be achieved with very high radiometric precision. The self-validation mode will be for radiance, sounding, and chemistry product validation of the routine larger area, higher frequency, spectra and geophysical products provided by the global and regional sounding and chemistry modes of operation

The expected sounding performance of GIFTS has been determined by radiance simulation. The results for the three example sounding modes of operation (Table 1) are shown in Figure 3.

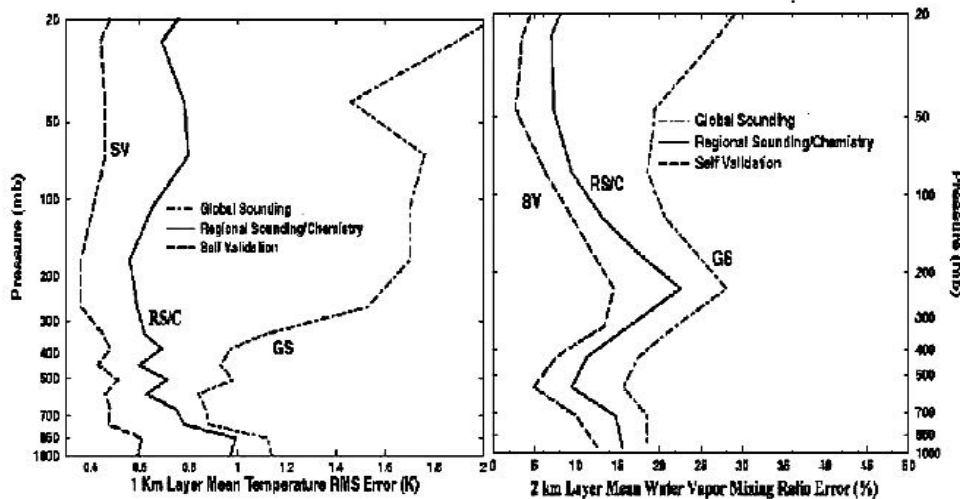


Figure3: Profile RMS errors for 3 GIFTS sounding modes of operation shown in Table 1 using expected radiometric noise performance

The radiometric noise and accuracy requirements for this retrieval of temperature and water vapor in the Regional Sounding and Chemistry mode with 10 sec dwell time are: (1) Noise Equivalent Radiance (NEN) in the LW spectral band ($685\text{-}1130\text{ cm}^{-1}$) $<0.2\text{ mW/m}^2\text{ sr cm}^{-1}$, (2) NEN in the SW/MW spectral band ($1650\text{-}2250\text{ cm}^{-1}$) $<0.06\text{ mW/m}^2\text{ sr cm}^{-1}$, and (3) Absolute calibration accuracy better than 1 K brightness temperature for Earth scene brightness temperatures $>190\text{ K}$ for the LW and $>240\text{ K}$ for the SW/MW band. Periodic views of onboard references and cold space will be used to realize this high calibration accuracy. Achieving these radiometric requirements for the primary high spectral resolution sounding mode is sufficient to insure the performance of other GIFTS imaging and sounding modes. The only other necessary constraints are that the time required to point the field-of-view to an adjacent region on Earth be less than 1 sec and that the pointing knowledge be better than 0.4 km for wind determination.

The GIFTS vertical resolution of CO and O₃ profiles is illustrated in Figure 4.

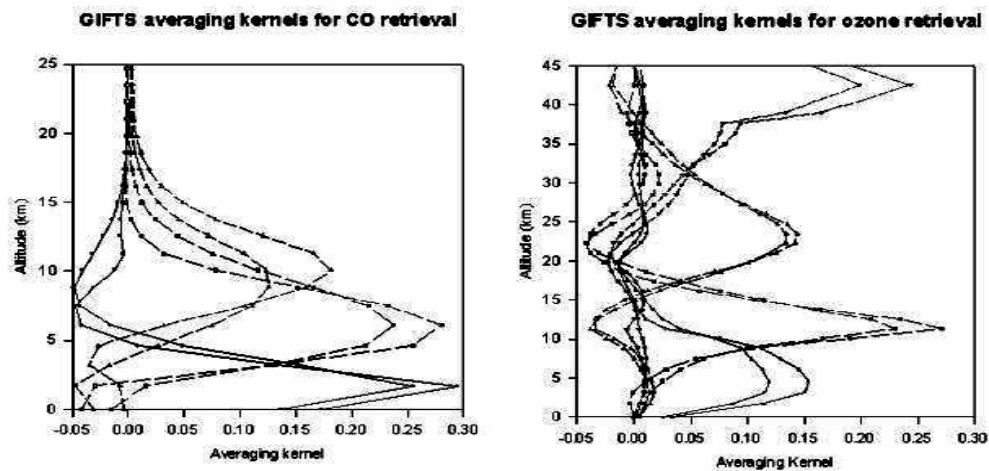


Figure 4: Vertical resolution functions for GIFTS retrieved carbon monoxide and ozone profiles at 0.6- and 0.3 cm^{-1} spectral resolutions, dashed and solid curves, respectively (courtesy of Nikita Pougatchev, CNU).

As shown, the GIFTS measurements of the time varying spatial distribution of CO and O₃ will be limited to a 3- to 11-km vertical resolution, decreasing with increasing altitude. The GIFTS capability to track vertically resolved trace gas concentrations together with the Water vapor winds is important for monitoring the global transport of pollutant gases resulting from biomass burning and industrial sources. Global Tropospheric Experiment (GTE) data have shown that this transport takes place at middle tropospheric levels⁶. Thus, GIFTS water vapor and trace gas motion sensing ability will provide a unique measure of chemical pollutant episode evolution and transport

3. Aircraft Demonstrations of Measurement Capability

A new high spectral resolution (0.25cm^{-1}) and high spatial resolution (2 Km) scanning (45 Km swath) interferometer sounding system, called the NPOESS Aircraft Sounding Testbed-Interferometer (NAST-I) has been built and flown to provide experimental observations needed to finalize the specifications and to test proposed designs and data processing algorithms for the Cross-track scanning Infrared Sounder (CrIS) to fly on the National Polar orbiting Operational Satellite System (NPOESS)^{6,7}. Because of the selection of the Geostationary Imaging Fourier Transform Spectrometer (GIFTS) to fly on the Earth Observing Three (EO-3) satellite, the data collected by the NAST-I has become an important source of information to test the design characteristics and data processing algorithms for that instrument as well. NAST-I is a passive infrared (IR) Michelson interferometer that scans the Earth and atmosphere from an aircraft such as the high-altitude NASA ER-2 research airplane (figure 5). The NAST-I, measures thermal radiation contiguously across the spectral region 3.5-16 microns with a spectral resolution of 0.25 cm^{-1} which is

sufficient for simulating the full spectral measurement capabilities of both the CrIS and the GIFTS. NAST also spatially scans the earth

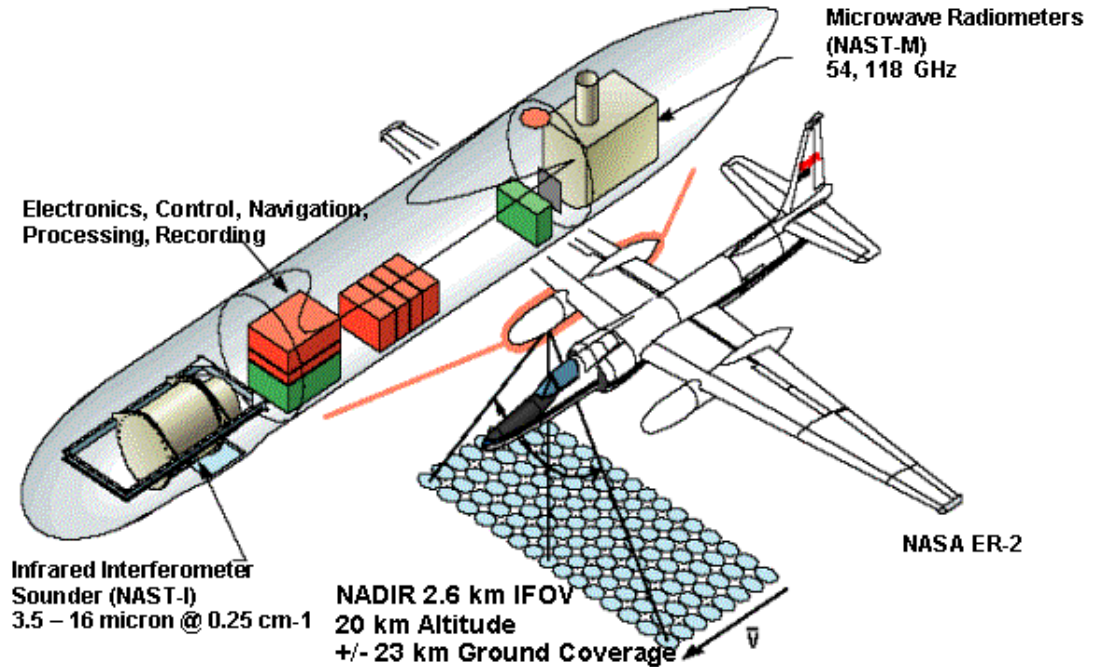


Figure 5: NAST-I Instrument Configuration on the NASA ER-2 Aircraft and Spatial Scan Geometry

beneath the aircraft with 3.0 km spatial resolution thereby providing three-dimensional images of spectral radiance, and derived products, similar to that to be obtained by the GIFTS. Unlike the gifts, however, the NAST-I does not use a large focal plane detector array to achieve its imaging capability, but instead, uses a cross-track scanning mirror and the motion of the aircraft to produce a similar result (figure 6). In any event, the NAST-I is the first interferometer instrument capable of imaging atmospheric temperature and

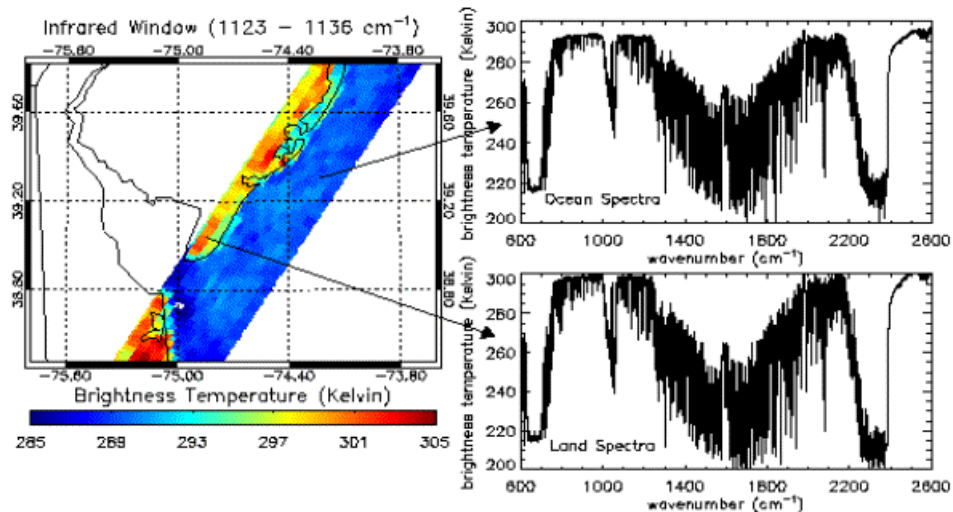


Figure 6: NAST-I observations along the Atlantic coastline near Wallops Island Virginia, July 11, 1998. Spectra are shown for two different 2.6 km. fields of view, one over land and one over ocean.

moisture with a very high horizontal resolution (~ 3 km, depending on scan angle). The NAST product is a three-dimensional "image" of the temperature and water vapor in the atmosphere at nearly a given moment in time. NAST-I provides a vertical resolution of 1 – 2 kilometers, so that 20, or more, distinct layers are

observed. As the ER-2 aircraft passes over the Earth, NAST scans an area of approximately 45 kilometers wide, at the earth's surface, collecting data on the properties of the Earth's surface and atmosphere beneath the aircraft. These data can be used to simulate the type of radiance data and derived geophysical products to be achieved from advanced polar and geostationary sounding interferometers, such as the CrIS and the GIFTS.

Temperature and moisture sounding capability with a hyperspectral resolution interferometer sounder has been demonstrated during numerous field programs with the NAST-I. The retrieval results to be shown were obtained using the eigenvector regression retrieval method⁸ as applied to high spectral resolution interferometer data⁹. In this technique, a training sample of historical radiosonde data is used to simulate radiance spectra for the NAST instrument. Eigenvectors are computed and regression equations which relate the eigenvector amplitudes to the radiosonde temperature and water vapor values are derived assuming a variable number of eigenvectors for the representation of the spectral radiance information. Appropriate random instrumental noise is then added to the simulated radiance data set and retrievals are performed for all cases as function of the number of eigenvectors. The optimal number of eigenvectors is then selected as that number which minimizes the RMS retrieval error for the historical radiosonde data set. This number ranges between 20 and 200, depending upon the variance associated with the historical data set used (such as regional or global, seasonal or annual). The regression equations for the optimal set are then applied to real NAST-I radiance measurements. Since all the radiative transfer calculations and eigenvector decomposition analysis is done "off-line" to the actual data processing, the algorithm is extremely fast when applied to real data. Because of both its speed and accuracy, the eigenvector retrieval method is planned to be used for the real-time processing of satellite GIFTS data.

Figure 7 shows a 75 km. cross-section of atmospheric temperature derived from NAST-I nadir viewing data obtained from the NASA ER-2 as it flew over the Andros Island Bahamas validation site during the CAMEX-4 experiment. As can be seen, fine scale horizontal structure of atmospheric temperature can be resolved. The agreement with a radiosonde released just prior to the overpass is in excellent agreement with the average NAST-I retrieval except in the tropopause region where the NAST data show significant horizontal variability.

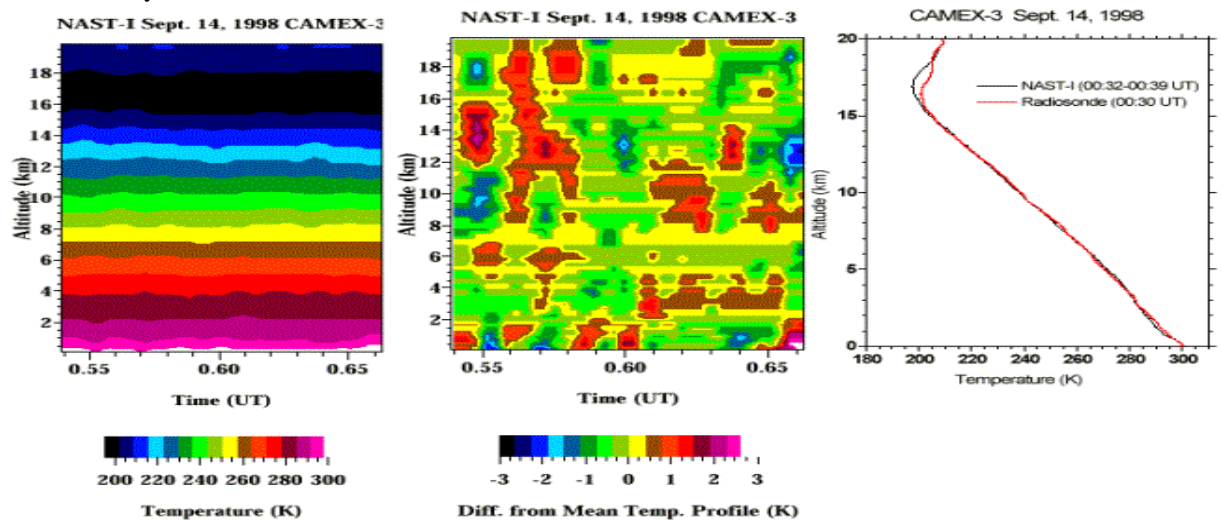


Figure 7: Cross-sections of atmospheric temperature and its horizontal deviation as observed with the NAST-I over Andros Island Bahamas, Sept. 14, 1998. A comparison with a validation radiosonde temperature measurement is also shown.

Figure 8. shows a similar cross-section for atmospheric relative humidity in the vicinity of Andros Island Bahamas. The spatial detail of the retrieved humidity distribution is particularly noteworthy. Most of the fine scale vertical details shown in the average radiosonde validation data are displayed by the NAST cross-section of soundings.

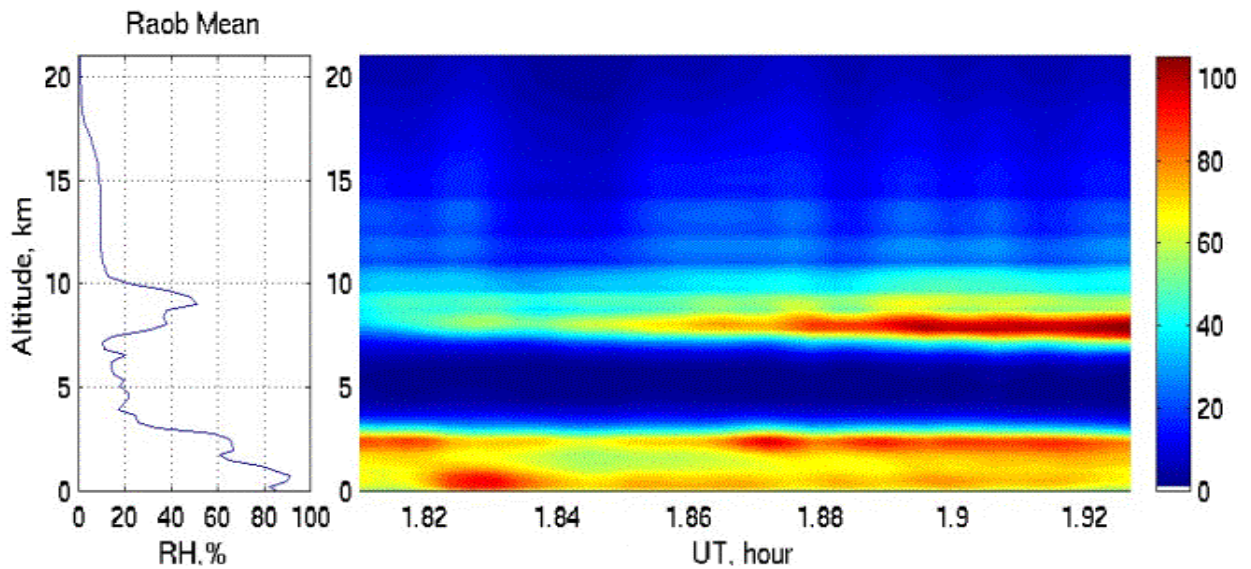


Figure 8: A 75 km. vertical cross-section of atmospheric relative humidity as observed with the NAST-I interferometer. A mean of four different radiosondes launched from Andros Island within two hours of the overpass time is shown for comparison.

Another comparison of NAST and radiosonde observed temperature and water vapor profiles is shown for measurements near International Falls (INL), Minnesota on March 21, 1999. The radiosonde was released at 23:30GMT while the NAST passed over the station twice, once at 22:40 GMT and then at 01:10GMT. Both comparisons are shown in figure 9.

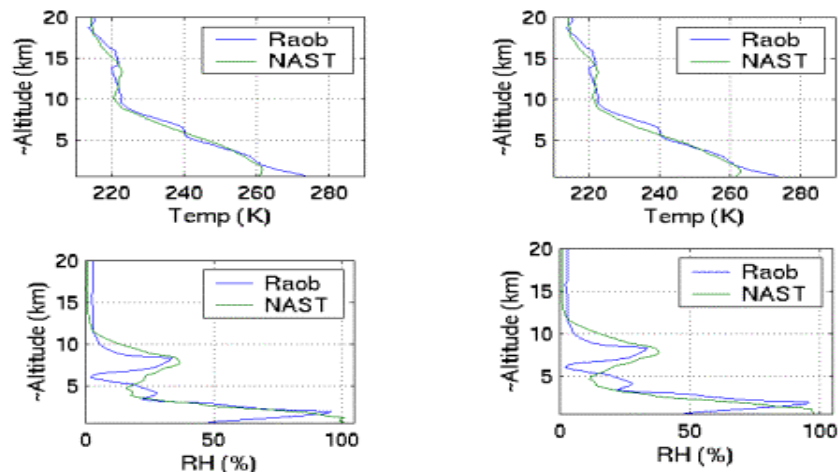


Figure 9: Comparisons of NAST retrievals at 22:40 GMT (left) and 01:10 GMT (right) with the 00:00 GMT International Falls Minnesota radiosonde observation

It is noteworthy that the ~2 km vertical resolution of NAST is not sufficient for capturing the finest scale vertical details observed by the point measuring radiosonde (e.g., the temperature inversion in the 6-7 km layer), although the larger synoptic scale details are resolved (e.g., the tropopause temperature structure and the moist layer in the 6-8 km layer). The time consistency of the NAST retrievals is also noteworthy. The disagreement near the surface is due to a cloud existing at the 2 km level. Because infrared radiation does not penetrate a dense cloud layer, the retrieval becomes isothermal below the cloud level and the humidity tends toward humidity in excess of 100% to produce profiles, which satisfy the radiative transfer

equation for the equivalent “clear” atmospheric condition assumed for the retrieval. One can see that the NAST indicated cloud top is very close to that displayed by the radiosonde humidity inflection point near 2 km, again illustrating the 1-2 km vertical resolution of the NAST soundings.

Another very dramatic illustration of NAST vertical resolution is displayed for a cross-section of atmospheric temperature, water vapor mixing ratio, and relative humidity obtained during a ferry flight from Wallops Island VA. to NASA Dryden Research Center in the Mohave Desert in southern California. The result is shown in figure 10. There are many noteworthy features in this cross-section including the strong thermal and humidity artifacts in the retrieved profiles produced below clouds as noted above for the INL comparison. Also, one can see that most of the flight is over clear skies with the lower atmosphere being warmer and less humid in the western part of the flight. There is a disturbance in the pattern of temperature and humidity near the Department of Energy (DoE) ARM-CART near 97 W longitude since here the aircraft deviated from a straight line track to perform a racetrack flight pattern over the CART site for validation purposes. In any event, one most interesting observation is the moisture outflow from a strong convective thunderstorm, which existed near 85 W longitude. The existence of the storm is strongly evident in the temperature and humidity profile artifacts retrieved from strongly cloud attenuated spectral radiance observations over the storm. What are most interesting, however, are the humidity observations in the clear air upstream and downstream from the convective cell. Note that moist air appears in two layers downstream east of the storm; one layer with a top near 300 mb (9km), which appears to be near the cloud top according to the temperature cross-section, and another at 100 mb (17 km) which is presumably near the tropopause level. Thus, these observations indicate that part of the moisture associated with the convection is being sheared away by the prevailing wind at the overall anvil altitude of the storm but a significant amount of moisture is being thrust into the tropopause region, possibly into the stratosphere, near the core of the convection. These observations clearly illustrate the potential value of the four dimensional moisture observations to be obtained with the GIFTS for understanding the thermodynamic consequences of intense convective storms.

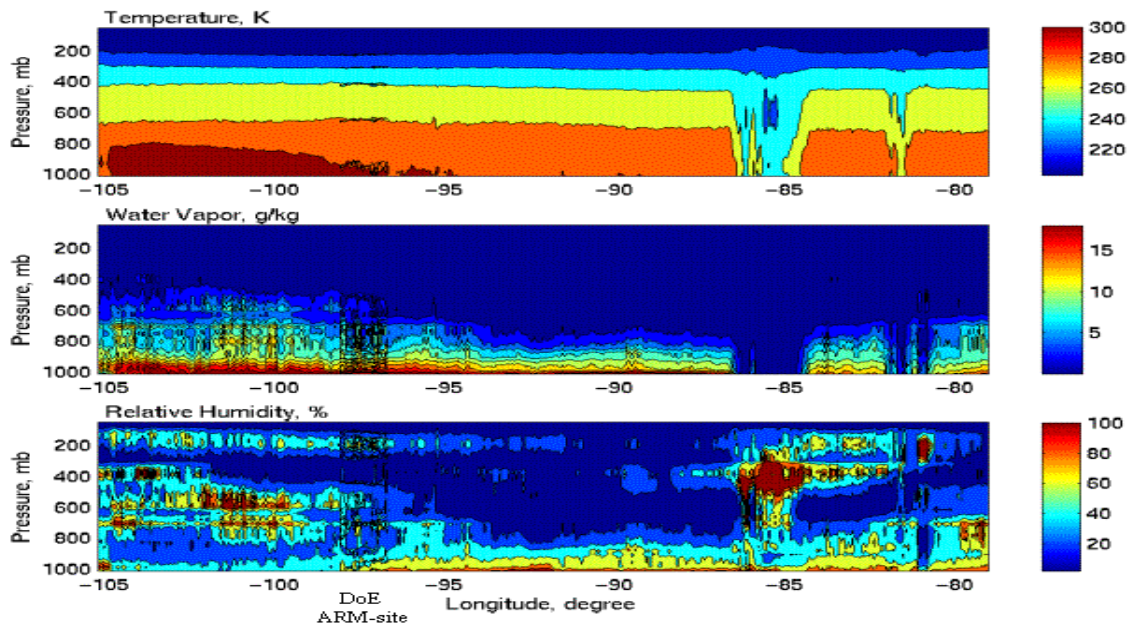


Figure 10: Vertical Cross-section of temperature, mixing ratio, and humidity derived from NAST Nadir view observations along the ER-2 flight track from Wallops Island VA. to Dryden CA.

Finally we present some examples of ozone profiles retrieved from NAST observations, using the eigenvector regression technique, in the vicinity of Wallops Island VA during 1998 and 1999. The statistics for the retrieval regression equations were obtained using more than 300 ozonesondes made from

Wallops Island VA. during a five year (1995-1999) time period. As shown in figure 11, the year to year differences in the upper troposphere and stratosphere revealed by the ozonesondes are also captured by the NAST retrievals; specifically, the decrease in ozone concentration in the 250-350 mb. layer, the increase in ozone in the 150 – 250 mb. layer, and the decrease in ozone in the 150 – 70 mb. layer. On the other hand, the year-to-year differences in the ozonesondes near the surface are not retrieved very well from the NAST data, although both the NAST retrievals and the ozonesondes show that the near surface ozone is greater for 1999 than for 1998. It is noteworthy that the location of the NAST data is over the Atlantic ocean, more than 200 km northeast of Wallops Island Va., limiting the agreement to be expected between these two independent ozone profile measurements, particularly near the surface where land-based pollutant sources of ozone exist.

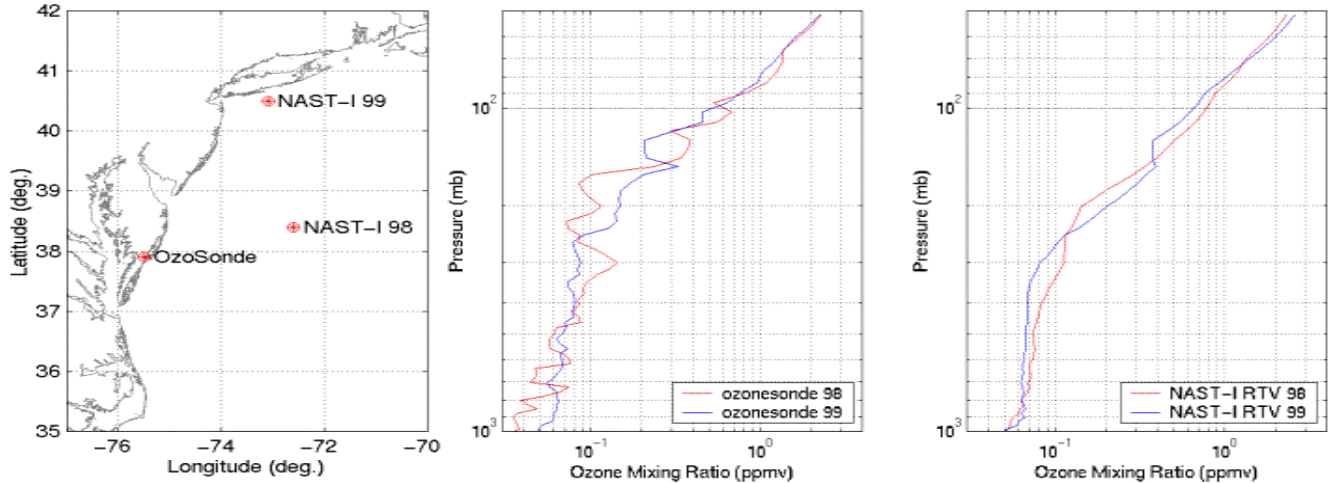


Figure 11: Ozonesondes at Wallops Island VA. And NAST ozone profile retrievals obtained near Wallops Is. (approximately 200 km northeast) for July 11, 1998 and August 23, 1999.

4. Summary

Hyperspectral radiance observations to be obtained from future satellite imaging Fourier transform spectrometers promise to provide revolutionary improvements in atmospheric measurements. Glimpses of the potential of these forthcoming data are already provided by measurements from the NPOESS Aircraft Sounding Test-bed high spectral resolution Fourier transform spectrometer being flown on the NASA ER-2, and more recently the Proteus, high altitude aircraft. Fast eigenvector regression retrieval methods, which are needed to keep up with the exceedingly high data rate of hyperspectral sounding systems, appear to be able to capture most of the vertical detail of atmospheric temperature and moisture structure contained in the high resolution radiance observations; preliminary results appear promising for the profiling of trace gases as well. In just a few years (2004), the first hyperspectral imaging spectrometer (GIFTS) will be orbited aboard a geostationary satellite to usher in a new era of high space and time resolution measurements of the atmosphere which will lead to a much better understanding of atmospheric processes and subsequently our ability to forecast weather and climate.

4. References

- ¹ Smith, W. L., H. B. Howell, and H. M. Woolf, 1979: The use of interferometric radiance measurements for sounding the atmosphere. *J. Atmos. Sci.*, 36, 566-575.
- ² Smith, W. L., H. E. Revercomb, D. D. LaPorte, L. A. Sromovsky, S. Silverman, H. M. Woolf, H. B. Howell, R. O. Knuteson, and H.-L. Huang, 1990: GHIS - The GOES High resolution Interferometer Sounder. *J. Appl. Meteor.*, 29, 1189-1204.
- ³ Stewart, T. R., C. M. Hayden, and W. L. Smith, 1985: A note on water vapor wind tracking using VAS data on McIDAS. *Bull. Amer. Meteor. Soc.*, 66, 1111-1115.
Sounder (HIS) observations. *J. Appl. Meteor.*, 29, 658-662.
- ⁴ Velden, C.S., C. M. Hayden, S.J. Nieman, W.P. Menzel, S. Wanzong and J. S. Goerss, 1997: Upper-tropospheric winds derived from geostationary satellite water vapor observations. *Bull. Amer. Meteor. Soc.*, 78, 173-195.
- ⁵ Pougatchev, N.S., 1999: PEM Tropics Carbon Monoxide Measurements in Historical Context. *J. Geophysical Research* (in press).
- ⁶ Cousins, D and W. L. Smith, 1997: National Polar-Orbiting Operational Environmental Satellite System (NPOESS) Airborne Sounder Testbed Interferometer (NAST-I). SPIE International Symposium on Optical Science, Engineering, and Instrumentation, San Diego, CA, 27 July - 1 August.
- ⁷ Smith, W. L. et al., NAST-I: results from revolutionary aircraft sounding spectrometer, *Proc. SPIE*, 3756, 2-8, 1999.
- ⁸ Smith, W. L., H. B. Howell, and H. M. Woolf, 1979: The use of interferometric radiance measurements for sounding the atmosphere. *J. Atmos. Sci.*, 36, 566-575.
- ⁹ Zhou, D.K., W.L. Smith, and A.M. Larar Temperature and Moisture Retrieval Algorithm Development for the NAST Interferometer. *Current Problems in Atmospheric Radiation*, A. Deepak Publishing, Hampton, Virginia.